GEOPHYSICS, VOL. 82, NO. 6 (NOVEMBER-DECEMBER 2017); P. B219–B230, 15 FIGS.
10.1190/GEO2017-0041.1

Case History

Integrated facies modeling in unconventional reservoirs using a frequentist approach: Example from a South Texas field

Reinaldo J. Michelena[1], Kevin S. Godbey[1], and Omar G. Angola[1]

ABSTRACT

Modeling of rock types or facies in unconventional reservoirs presents numerous challenges that are not encountered in conventional reservoirs. Because the exploitation of unconventional reservoirs frequently relies on the use of large numbers of long, data-poor horizontal wells, routine tasks in conventional reservoirs, such as petrophysical analyses and rock-physics diagnostics, become problematic in unconventional reservoirs due to insufficient data. Similarly, the inability to generate synthetic seismograms in the horizontal section of the wells makes seismic well ties and time-depth conversions more difficult. Our approach for facies modeling in unconventional reservoirs attempts to overcome these challenges by using the abundant log information available along the vertical pilot well to extract discrete facies indicators (facies flags) from logging-while-drilling information along the horizontals. After performing a time-depth conversion constrained by geosteering information, we estimate facies probabilities using facies flags and prestack elastic inversion results also extracted along the horizontals. As opposed to the Bayesian formalism commonly used for facies probabilities estimation, our frequentist approach estimates probabilities directly from proportions derived from crossplots of inverted elastic properties without using the Bayes formula. No prior information is required. The margin of error in the probabilities is also estimated by applying a well-known formula used to estimate the margin of error in opinion polls. Finally, we use seismic probability results to select only points with high probability and high reliability, which are treated as hard constraints for stochastic facies modeling. The selection of the seismic constraints is also weighted by the vertical facies trend expected for the area of interest. Our final facies model closely follows horizontal and vertical well facies data, vertical proportion curves, and selected seismic constraints. The application of the methodology is illustrated in a carbonate-rich, unconventional reservoir in South Texas.

INTRODUCTION

The development of unconventional reservoirs requires large numbers of closely spaced wells aimed to maximize recovery in rocks of very low permeability that can produce commercial hydrocarbons only after hydraulic stimulation. Multiwell drilling from a single pad, which can handle more than a dozen horizontal wells, has become the norm to develop producing intervals. Log data available in horizontal wells typically consist of gamma ray (GR) and mud logs obtained while drilling (LWD) to steer the well paths along the target, and they are therefore biased by design toward sampling the more productive rocks. Other logs are rarely recorded along horizontal wells. For thin-producing intervals, the number of vertical wells with a complete set of logs is much smaller than the number of horizontals because vertical wells are mainly used to identify the target depth for future horizontals and to monitor reservoir pressure. Many multiwell pads can also be designed without the help of nearby vertical wells, and geosteering relies entirely on LWD tools. Typical lengths of horizontal sections range between 1 and 3 km, long enough to observe changes in rock properties,

First presented at the SEG 86th Annual International Meeting. Manuscript received by the Editor 18 January 2017; revised manuscript received 9 June 2017; published ahead of production 31 July 2017; published online 25 September 2017.
[1]iReservoir.com Inc., Littleton, Colorado, USA. E-mail: michelena@ireservoir.com; godbey@ireservoir.com; oangola@ireservoir.com.

saturations, and thicknesses away from the pilot well. These data disparities between abundant wells with long horizontal sections and scarce vertical wells create new challenges for 3D facies mapping that are not common in conventional reservoirs.

The use of geostatistical facies mapping methodologies has been common practice in the oil and gas industry for more than two decades due to the importance of rock facies as building blocks for reservoir models (Jordan and Goggin, 1995). Because stationarity is a central hypothesis in most of these methodologies, the challenge for geostatistical methods has been the introduction of spatial trends in the models that handle nonstationarity adequately, as indicated by Yarus et al. (2012). In this regard, log data, seismic data, and other geologic trends are often used to constrain the spatial variability of facies in the geostatistical modeling tools commercially available today.

Understanding the spatial variability of facies in unconventional reservoirs is important for a variety of reasons. Facies not only help to map variations in matrix properties, such as porosity and permeability, but they also help to assess whether a rock will fracture under hydraulic stress (brittleness). Besides, facies also control the variability and intensity of existing natural fractures in the vicinity of faults.

The standard geophysicist's workflow for facies mapping in conventional reservoirs using seismic data starts by performing crossplots of elastic properties at the log scale colored by petrophysical properties. Then, these crossplots are used to create probability density functions (PDFs) for different facies whose elastic properties are expected to be well-separated in the elastic domain (Mukerji et al., 2001). PDFs are used in a Bayesian context to estimate facies probabilities using the inverted elastic properties in the volume of interest. PDFs can also be derived from upscaled log data or inverted seismic results extracted along the well path. Prior facies probabilities are required in the Bayesian approach and can have a strong influence on the final results. These prior probabilities, however, are not routinely checked to make sure they are actually honored by the final results, in particular, when the domain of application of the process is the seismic volume. An exception to this rule occurs when using geostatistical inversion in geologic grids (i.e., a grid that follows the stratigraphy, unlike a regularly spaced 3D seismic volume). Sams et al. (2011) show that geostatistical inversion allows the use of prior probabilities as a constraint for facies modeling after assigning unique statistical and geostatistical properties to each facies.

In the framework of geologic modeling, prior facies probabilities trends derived from log facies data are called vertical proportion curves (VPCs) (Ravenne et al., 2002). VPCs are histograms of lithofacies for layers parallel to a reference level that capture vertical trends in the data. They may be used to describe the sequential evolution of the interval of interest and/or to quantify the likelihood of lateral continuity of facies within a given layer (if enough wells are available). In contrast to the geophysicist's workflow that does not attempt to honor the VPC when mapping facies, the geologic modeler's (geomodeler) workflow for facies mapping typically focuses on honoring well facies data as well as the VPC, but it leaves the lateral variability in the interwell region to conceptual geologic trends. Geostatistical inversion of seismic data for facies and continuous elastic properties (Saussus and Sams, 2012) is again an exception to this rule because it attempts to bring the geophysicist's and geomodeler's approaches together into a single step. The domain of computation of Saussus and Sams' (2012) approach is a geologic grid; it uses predictive rock-physics models to relate seismic properties and facies properties, and it attempts to honor all areal and vertical (VPC) probability trends in the final reservoir model.

The works of Mukerji et al. (2001), Sams et al. (2011), and Saussus and Sams (2012) are a few examples of the two general approaches of reservoir modeling constrained by seismic data explained by Grana et al. (2012): multistep inversion and stochastic inversion. For more detailed references and descriptions of how these approaches are applied to the problem of facies and rock-property modeling, the reader is referred to the "Introduction" section of Grana et al. (2012).

The application of facies mapping workflows designed with conventional reservoirs in mind is not straightforward in unconventional targets. As mentioned above, the geophysicist's workflow requires collocated, log-scale elastic and petrophysical information to generate or calibrate PDFs and rock-physics models. Because this information is usually not available along horizontal wells, geophysicists are forced to leave behind abundant GR and mud log data that carry useful information about the target interval along possibly tens of kilometers of lateral sections. By doing so, the seismic calibration with log data is then limited to whatever can be extracted from a few hundred meters of log data along the vertical pilot well, which may or may not be representative of the variability observed along the laterals. Situations in which vertical pilot wells are not available are not uncommon. Another difficulty for geophysicists is that facies in unconventional reservoirs typically show significant overlap of elastic properties, and no estimate of error is provided in the Bayesian approach when picking the most likely between comparable probabilities.

For geomodelers, the situation is also challenging. Facies information cannot be honored along horizontal wells because this information is commonly not extracted from LWD GR and mud log data. Even if facies data were available, VPCs are difficult to generate from horizontal wells and the lateral continuity of the facies between undulating horizontal wells is hard to assess. Under these circumstances, geomodelers are only left with the facies data along the pilot well and possibly conceptual geologic trends to constrain their facies models.

We present in this paper a workflow and example of application of facies modeling in unconventional reservoirs that attempts to overcome these difficulties. We start by calibrating the GR log along the pilot well with facies information derived from a complete set of logs (GR, resistivity, compressional sonic, dipole sonic, porosity, water saturation, and fractions of calcite, quartz, illite, and kerogen). This log-scale facies model is then used to extract facies information along the horizontal wells. Because no elastic logs are available along the horizontal wells, elastic information is extracted from prestack inversion results of conventional P-wave seismic data along the well trajectories. This information is used to estimate facies probabilities from crossplots of inverted elastic properties (acoustic impedance and V_P/V_S ratio) colored by discrete facies indicators (facies flags). The proportions of sampled facies along the horizontals are used to estimate the probabilities for the larger volume using a poll-like, frequentist method. Our method fundamentally differs from commonly used Bayesian approaches for facies probability estimation in the way prior information is handled. A by-product of the facies probability estimation is a measure of reliability of the estimates that is based on the standard for-

mula for margin error in opinion polls. Probability and reliability information is then used to select points from the probability volumes that are treated as hard constraints for geostatistical facies modeling. The goal of the modeling is to honor prior information, such as VPC at the vertical pilot well, dominant facies information along the horizontals and pilot well, and hard constraints extracted from the seismic. The application of the workflow is illustrated with a pad-scale example from a Cretaceous-age, carbonate unconventional reservoir in South Texas (Figure 1). For the sake of brevity, we will omit detailed explanations of steps that have become routine practice in reservoir characterization, such as log normalization, petrophysical modeling, petrophysical/geologic facies definition, and prestack seismic inversion. Instead, we will focus on the new elements of the proposed workflow and how they are integrated with results from well-known methodologies.

LOG-SCALE FACIES MODELING

The interval of interest for this study is approximately 60 m (200 ft) thick and consists mostly of carbonate facies (porous packstone, porous mudstone, and tight carbonate) with a small proportion of kerogen-rich clay layers. These clay layers are located mostly in the deeper portion of the interval, and they are not considered a target for horizontal drilling in the area. These facies were defined by petrophysical analyses in the pilot well, and they were calibrated with core data (not shown). Petrophysical analyses included neutron-density crossplots and multimineral modeling for fractions of minerals and fluids. The relative proportion of facies in the pilot well is 53% packstone, 19% mudstone, 21% clay, and 7% tight carbonate. The mineral composition of these facies is calcite, quartz, illite, and kerogen. Fractions of these minerals were estimated by petrophysical forward modeling along with fractions of hydrocarbon and water. Calcite is the dominant mineral. Within the calcite-rich matrix, more quartz and illite is associated with mudstone, and less quartz is associated with packstone. Tight facies are low-porosity rocks and tend to have very little quartz and clay. Experience of the company that operates the field indicates that brittleness is proportional to calcite content and decreases with clay content. Therefore, as a general rule in this area, we can say that the highest brittleness corresponds to tight carbonates followed by packstones, mudstones, and clays, respectively.

Detailed facies information (packstone, mudstone, clay, and tight carbonate) could only be extracted along the pilot well. Along the eight horizontal wells, the only digital information available for this study was LWD GR and mud gas logs. No other wireline logs or qualitative rock descriptions from mud logs were available either. Therefore, if we want to use LWD GR logs along the horizontals to calibrate seismic data, we first need to examine the relations between the wireline GR and facies along the pilot and then relate such logs to the LWD GR along the horizontals. Before comparing LWD GR logs with wireline GR logs, we first need to normalize them to make sure that similar rocks show similar GR responses. Figure 2a shows the wireline GR response of different facies along the pilot well. After testing different normalized GR cutoffs, we selected 70 American Petroleum Institute (API gamma ray unit) as the most adequate to separate more brittle from less brittle facies along the pilot well. Notice that we have used the term "facies" to refer to the lithologic indicators packstone, mudstone, clay, and tight carbonate as well as the more general brittle/less brittle classes. Although they are correlated, one cannot be fully determined by the other. As the pie charts in Figure 2a show, for GR less than 70 API, 98% of the facies are brittle carbonates, whereas for GR greater than 70 API, 65% of the facies correspond to ductile clay. As we will discuss later, this GR cutoff is selected iteratively with the seismic calibration to make sure that we also improve the separation or clustering of facies in crossplots of inverted elastic attributes. Figure 2b shows the histogram of LWD GR logs along the horizontals with the 70 API cutoff indicated as a reference. Figure 3 shows the final brittle and nonbrittle facies along the horizontal wells.

CALIBRATION OF INVERTED ELASTIC PROPERTIES

Once facies have been defined along the horizontal wells, we need to understand their relation to the elastic properties of the reservoir before seismic data are used to map the variability in the interwell region. The only elastic information available along the horizontal wells was the acoustic impedance and V_P/V_S ratio from a prestack inversion of seismic data (Figure 4) that was available prior to this study. The inversion was the result of a conventional model-based approach and was considered of average quality after comparing with well data along the pilot well (Figure 5). The interval of interest shows low acoustic impedance and V_P/V_S ratio values embedded in otherwise high values. This high contrast in elastic properties with the surrounding formations makes more difficult the estimation of impedances from seismic data in the entire

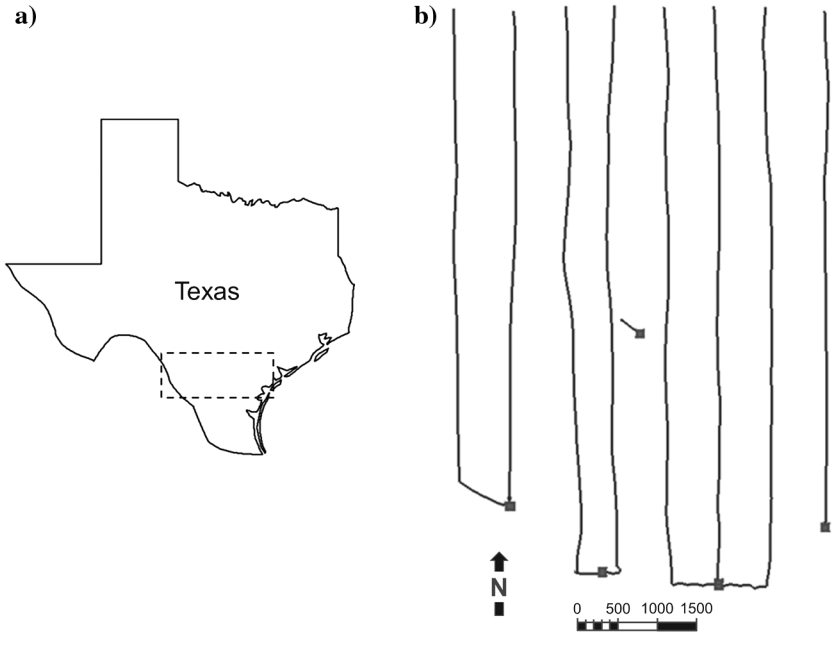

Figure 1. (a) Approximate location of the study area (dashed rectangle). (b) Relative locations of wells used in this study: one vertical pilot well near the middle and eight horizontal wells in its vicinity. The scale is in feet. Lateral sections range between 1820 and 2210 m (6000 and 7300 ft).

interval of interest. The maximum frequency in the background model was approximately 12 Hz.

Before extracting inverted attributes along the well paths, we first converted the seismic information to depth by using the seismic-well tie along the pilot and geosteering data as control points. Drillers steer the borehole position by using LWD GR and mud logs to make sure it stays on target. If it does, we check that the relative trajectory of the well with respect to the top and base of the interval of interest is consistent with this observation. We also honor selected formation tops interpreted along the well path to make sure that the top and base horizons follow the expected dips in the depth domain. Additional control points acting as tops along the well paths may be needed to better constrain horizons in depth. Assumptions about the thickness of the interval of interest along the well paths may also be necessary in the absence of actual formation tops. The whole process is time consuming because typically every well has to be fixed individually and tens (or hundreds) of wells may be involved. After this process, there is still no guarantee that the relative positions of wells and seismic data will have accuracy obtained from seismic-well ties using synthetic seismograms in vertical or slightly deviated wells. In the example presented in this paper, we tested two plausible velocity models that resulted in similar calibrations of the seismic data with facies flags. The low resolution of the seismic data within the 60 m (200 ft) interval of interest explains this similarity between the two calibrations. The selection of the final velocity model for the study was based on other geologic and engineering considerations. If time-depth conversions are not performed carefully, we will likely see horizontal wells either out of zone or crossing horizons that they are not expected to cross.

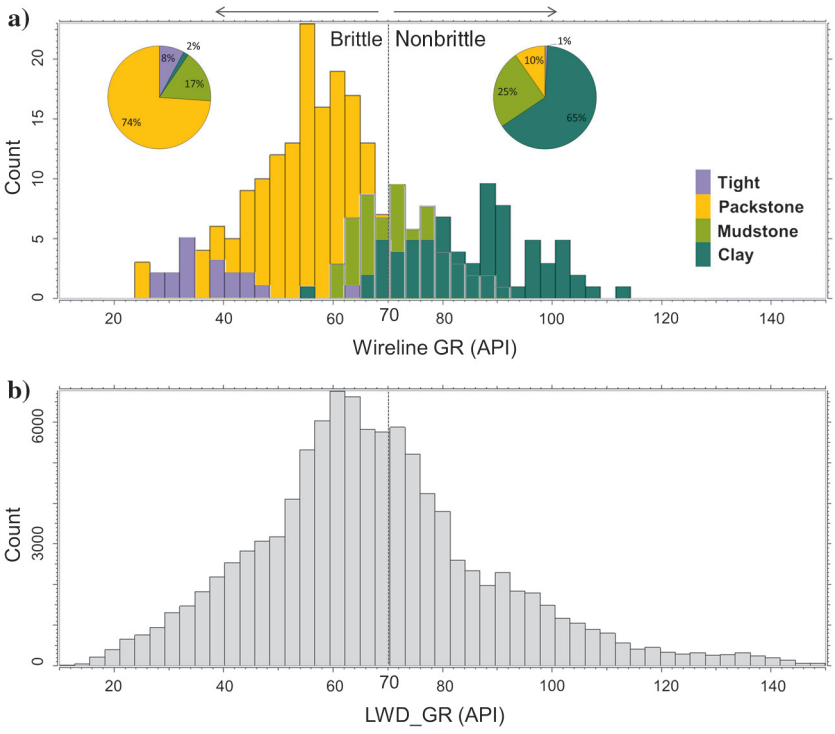

Figure 2. (a) Histograms of wireline GR along the pilot well for different facies. The relative proportion of the original facies in each GR region is indicated by the pie charts. (b) Histogram of normalized LWD GR along the eight horizontal wells in the area of interest.

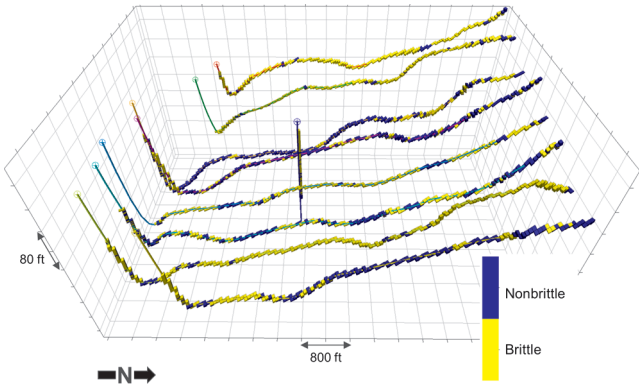

Figure 3. Brittle and nonbrittle facies extracted from normalized LWD GR logs. The pilot well is indicated by a "+." Notice how some wells navigate large portions of brittle rock, whereas others do not. Lateral sections range between 1820 and 2210 m (6000 and 7300 ft).

After time-depth conversion, we mapped the results from the seismic volume of $30 \times 30 \times 1.5$m ($110 \times 110 \times 5$ ft) cell size onto a finer geologic grid of approximately $15 \times 15 \times 0.6$ m ($50 \times 50 \times 2$ ft) cell size. Although the dominant cell thickness is approximately 0.6 m (2 ft), the actual distribution of cell thicknesses varies between 0.3 and 0.9 m (1.0 and 3 ft) to adapt for the variations in dip and thickness between the different horizons. In this case, the mapping was performed by doing nearest-neighbor interpolation plus smoothing from the seismic cells to the grid cells. The orientation of the axes of the geologic grid was determined by the orientation of the maximum horizontal stress. Elastic attributes were extracted along the well paths using the same sampling interval of the LWD GR logs (0.3 m or 1 ft).

Because inverted elastic properties and log facies data are now collocated (Figures 3 and 4), we can make seismic scale rock-physics crossplots to understand the relation between these variables for different LWD GR cutoffs. As explained above, a 70 API GR cutoff was adequate to separate brittle from nonbrittle facies at both scales. Figure 6a shows the crossplot of inverted elastic properties extracted along the horizontals colored by log brittle/nonbrittle facies flags. This result indicates that less abundant nonbrittle facies tend to cluster in areas of lower acoustic impedance and overlap with dominant brittle facies at a seismic scale. For comparison purposes, Figure 6b shows the log-scale crossplot of the acoustic impedance versus V_P/V_S ratio along the pilot well for the target interval. This figure confirms that at log scale, brittle facies also show higher acoustic impedance than nonbrittle facies, as observed at seismic scale along the horizontal wells. Figure 6c shows the crossplot of inverted elastic properties extracted along the pilot well. No significant clustering or separation of facies is observed, which indicates that, in this

case, even though the quality of the inversion results is reasonably good for the entire inverted interval (as shown in Figure 5), the results within the interval of interest along the pilot well are not representative of the actual relations between the facies and the inverted elastic properties in a larger area. The large number of samples along the horizontal wells yields a seismic/facies calibration that is closer to what we expect from log data as compared with using only inverted data along the pilot well.

SEISMIC-SCALE FACIES PROBABILITIES

In the previous section, we showed that brittle and nonbrittle facies tend to cluster in regions that may or may not overlap in the crossplot of inverted elastic properties. In this section, we explain how we can translate this observation into quantitative facies probabilities. Although the method for probability estimation from inversion results used in this paper was already described by Michelena et al. (2011) and illustrated in a tight gas reservoir with a large number of vertical wells, we will revisit this method here in the context of opinion polls (formally, Bernoulli, or binomial trials). This new perspective will help us to borrow some concepts from this field to better understand the problem of facies probability estimation. Although we emphasize the use of inverted elastic properties, any other seismic-derived attribute can be used as long as its relation with the facies can be demonstrated by using crossplots.

We start by crossplotting the 3D grids of inverted acoustic impedance and the V_P/V_S ratio as shown in Figure 7a. Each sample in the 3D grid is represented by a gray dot in the crossplot. Each dot is considered an individual, and the size of the "population" is the

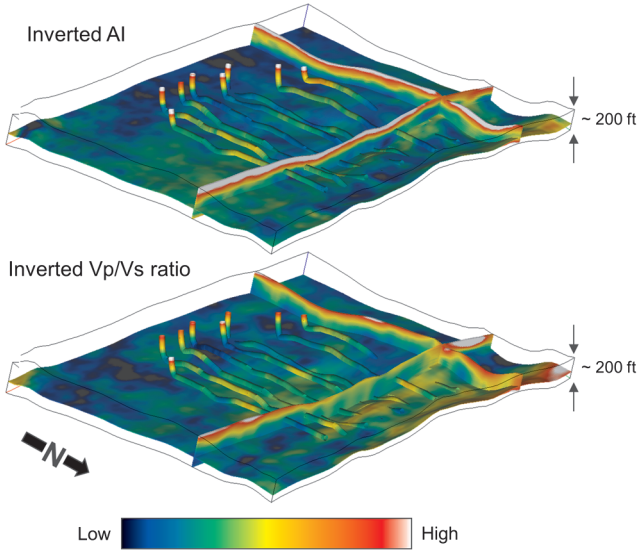

Figure 4. Inverted acoustic impedance and V_P/V_S ratio mapped to a geologic grid in the depth domain. This information is also extracted along the horizontal wells for further calibration with facies flags. Lateral sections range between 1820 and 2210 m (6000 and 7300 ft).

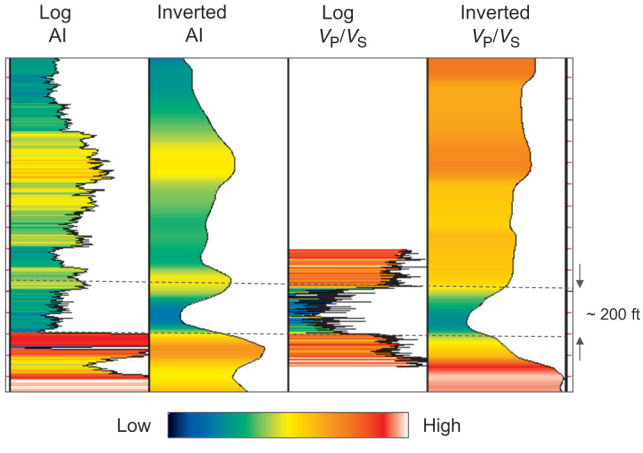

Figure 5. Inversion results along the pilot well compared with log data. The interval of interest is indicated by the dashed lines. Both AI curves are plotted at the same scale. The same is true for the V_P/V_S ratio curves. The colors represent the same information as the curves.

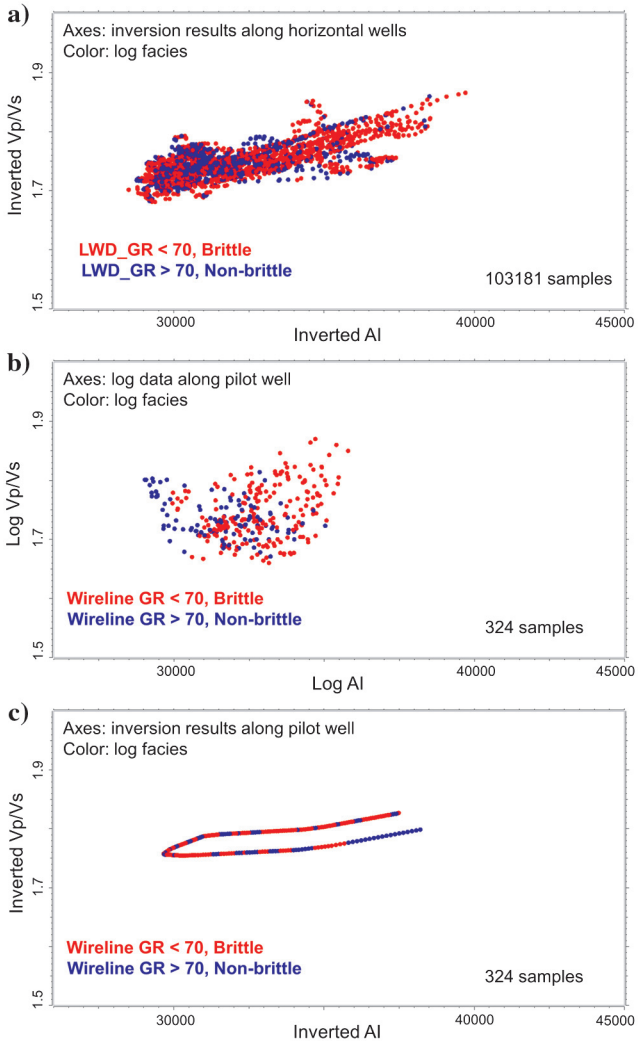

Figure 6. Crossplots of acoustic impedance versus V_P/V_S ratio colored by log-scale facies. (a) Using inversion results extracted along eight horizontal wells and coloring by facies generated from LWD GR logs. (b) Using the log acoustic impedance and V_P/V_S ratio along the pilot well and coloring by facies generated from the wireline GR along the pilot (Figure 2a). (c) Using inversion results extracted along the pilot well and coloring by facies generated from the wireline GR log.

number of samples in the volume (which may be in the order of millions). The map of the "country" where the population "lives" is the area covered by the gray points of the crossplot. The country can be divided into states (grid cells in the crossplot, Figure 7a). Ideally, if we want to poll the population about a particular subject, we select and interrogate a subset of individuals (sample) to estimate from their answers the characteristics of the whole population. The selection of such individuals is usually a careful process that aims to make sure that the selected sample is representative of the entire population. In our problem of facies probability estimation, we can only interrogate individuals that live along the well paths (Figure 7b) and the question we ask is: "Will you vote for brittle or nonbrittle?" The answer to this question is given by the facies flag that corresponds to that individual along the horizontal well path (Figure 7c). Because the samples along the well paths live in different states (grid cells), we then assume that the proportion of the answers within the boundaries of each state is representative of the entire state. In other words, the proportion of brittle or nonbrittle facies calculated from the samples within a state is assumed to be the probability of that facies for all the population in the same state across the whole seismic volume. This is how opinion polls work.

If we pose the problem of facies probability estimation in the context of opinion polls, we may conclude that our poll is a poorly designed one because we do nothing to make sure that the selection of the samples is representative. On the contrary, horizontal well data are biased toward good-producing facies and may under-sample or ignore other rocks that are critical to understand nonproducing facies. Since, in general, wells are not drilled with the purpose of acquiring information, this limitation is not exclusive to our method. Because we have no choice, we will assume that facies sampled along tens of kilometers of horizontal wells across different states (grid cells) are still a useful representation of the entire population within the geologic interval of interest.

To address the problem of under-sampling of ranges of inverted elastic properties by well data, we perform probability estimation using cells (states) of different sizes to partition the crossplot of elastic properties. First, we select the area for probability analysis in the crossplot as indicated by the red rectangle in Figure 7c (we will explain later how the area outside is handled). Then, we divide that area in 4 (2×2) cells and compute the proportions of brittle versus nonbrittle facies in those cells. This gives us a first-pass coarse probability estimate for all attribute ranges regardless of whether they are actually sampled by well data, analogous to giving poll results in four regions of a country (e.g., northwest, northeast, southeast, and southwest) even if some particular states within those regions

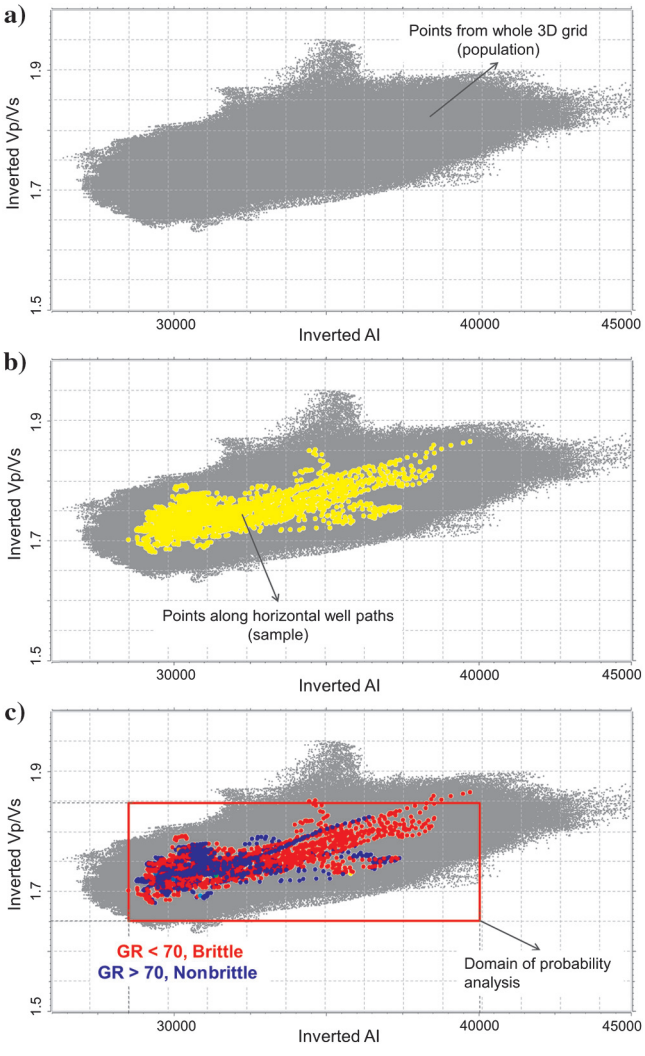

Figure 7. (a) Crossplot of acoustic impedance versus V_P/V_S ratio using all points in a 3D grid (entire population) and partitioned into grid cells (states). (b) Samples along the well paths (yellow) relative to the entire population. (c) Facies flags along the well paths (the same as Figure 6a).

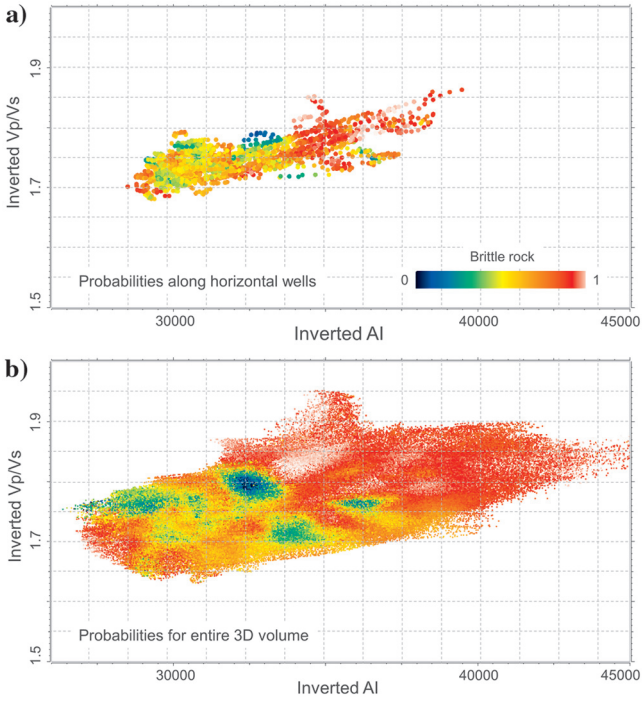

Figure 8. Crossplots of inverted elastic properties colored by probability of brittle facies. (a) Result of multiresolution probability analysis for the samples along the horizontal well paths. These probabilities agree with the facies flags along the well paths shown in Figure 6a. (b) Probabilities mapped to a 3D grid after multiresolution analysis and interpolation in (x, y, z) domain.

were not actually polled. Then, we divide the area of analysis into 25 (5 × 5) cells and compute again proportions of brittle versus nonbrittle. These new higher resolution proportions overwrite the original coarse proportions wherever new proportions are calculated in areas with a usable number of samples. The multiresolution process continues by dividing the area of analysis in finer cells and overwriting the previous proportions in which new proportions can be calculated. In the examples presented in this paper, we divided the crossplot in 4, 25, 100, 625, and 2500 cells, which allowed a good representation of coarse and fine-scale proportions. These proportions are then used to estimate facies probabilities for all acoustic impedance and V_P/V_S ratio discrete intervals that fall within the area of analysis (red rectangle in Figure 7c). Notice that not all gray points within the red rectangle of Figure 7c are sampled by well data. The multiresolution analysis provides a way to estimate probabilities for all points such that points far from the well data (in the crossplot domain) will tend to honor more global (coarse resolution) statistics, whereas points closer to the well data (in the crossplot domain) will tend to honor the finer variability sampled along well paths.

Once we map the probabilities estimated within the red rectangle to the 3D grid, we still need to classify points that fall outside the rectangle. We do this by either interpolating probabilities in the (x, y, z) space domain or by using conceptual, rock-physics-based prior information about end member facies.

Figure 8a shows the final proportions estimated along the well paths in the crossplot domain, and Figure 8b shows the final probabilities in the whole 3D grid after multiresolution probability analysis and interpolation in the space domain. Figure 9 shows there is good agreement between estimated facies probabilities (black) and expected facies flags (yellow) along the horizontal well paths. Notice the enhanced resolution in the probability results when compared with the inverted acoustic impedance (third track). Similar results are obtained when comparing against the inverted V_P/V_S ratio, which has similar resolution to the inverted acoustic impedance (Figure 5). The increased resolution of the probability estimates results from incorporating the log-scale data into the analysis using a fine discretization of the inverted attributes.

In our approach, the information extracted from the crossplot is the discrete proportion of brittle facies for the ranges of attributes sampled by the well paths. This proportion is used to approximate $P(F|A)$ (where F is the facies and A is the attribute), that is, the probability of a facies given the attribute. As Figure 8 shows, these proportions can be later used to estimate probabilities in the entire volume. No additional corrections are required. On the contrary, the information extracted from the crossplot of elastic properties in the approach proposed by Mukerji et al. (2001) is the probability of the attribute given a facies $P(A|F)$. This probability is later transformed into $P(F|A)$ by using the Bayes formula as follows:

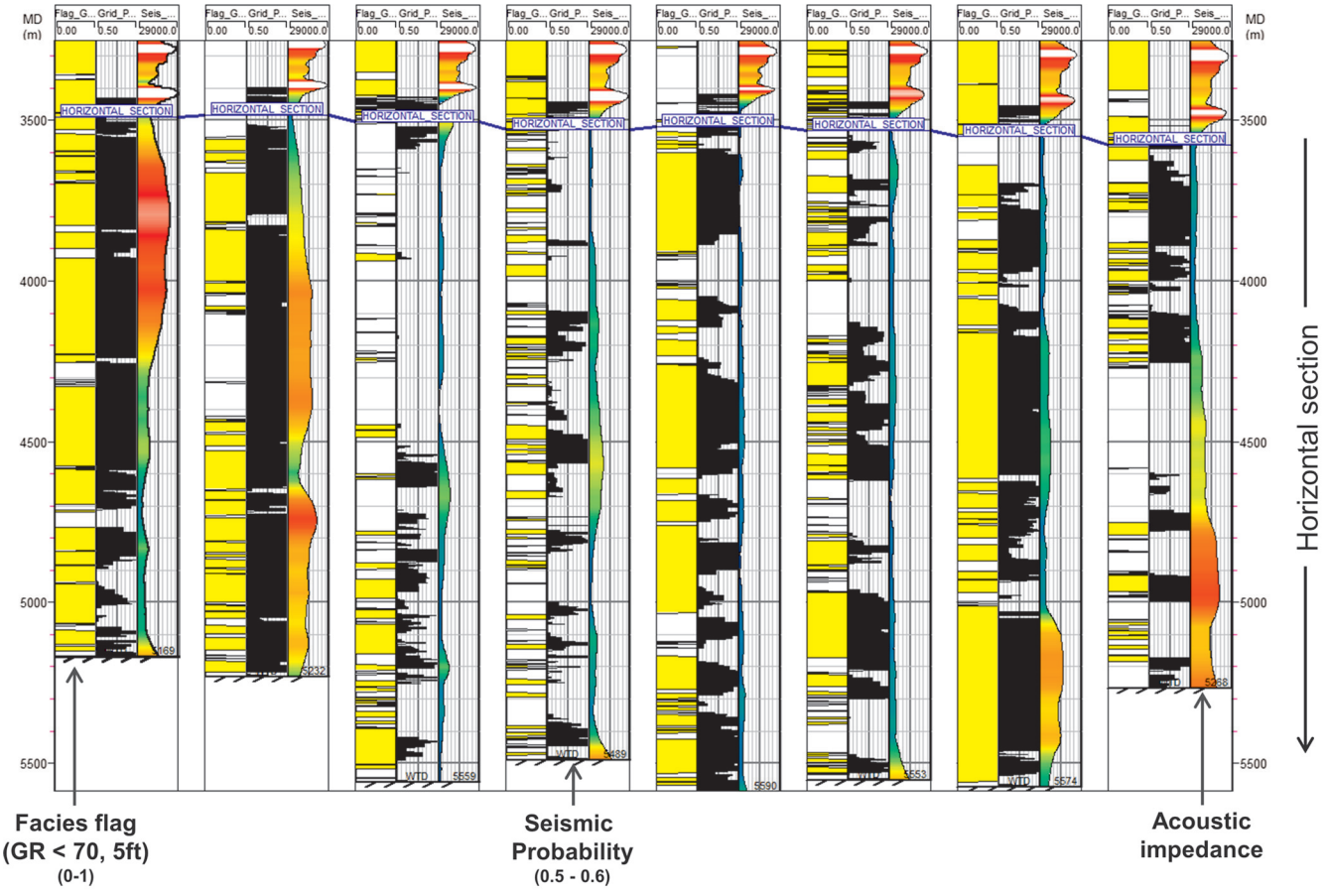

Figure 9. Comparison of estimated facies probabilities of brittle rock (black) versus expected brittle facies flags (yellow) derived from LWD GR log along lateral sections. The third track in each well is the inverted acoustic impedance extracted along the horizontal sections.

$$P(F|A) = \frac{P(A|F)P(F)}{P(A)}, \quad (1)$$

where $P(F)$ is the prior facies probability and $P(A)$ is the probability of the attribute. Although our methodology focuses on the direct estimation of the left side of Bayes formula, Mukerji et al. (2001) work on the right side of the formula by first estimating continuous PDF for $P(A|F)$ and then transforming these functions into $P(F|A)$ using $P(F)$, $P(A)$, and Bayes' formula. Because the estimation of $P(F|A)$ requires the use of Bayes' formula, the latter approach is classified as Bayesian. Our approach, on the contrary, does not need to invoke the Bayes formula because the estimation of $P(F|A)$ is based on proportions (or statistical frequencies) calculated directly from the data. For this reason, our approach is classified as frequentist. Many years of discussions among statisticians about the merits of Bayesian and frequentist approaches for statistical inference have not been exempted from controversy (see e.g., the work of Bayarri and Berger, 2004). However, our purpose in this paper is not to elaborate on the controversy; it is simply to present an alternative based on a different set of assumptions to the commonly used Bayesian inference for facies probability estimation.

The polling question "brittle or nonbrittle?" falls into the category of binomial experiments in which we can choose only between two answers. In the case of more than two facies, the proportions for each can be estimated by considering "This facies or not this facies?" type questions. If we assume that the sample is large enough, we can estimate the margin of error of the sample proportion of binomial experiments by using the Wald interval, a well-known expression among public opinion pollsters (Brown et al., 2001):

$$\text{Error} = \pm Z\sqrt{\frac{p(1-p)}{n}}, \quad (2)$$

where p is the estimated proportion, n is the number of samples, and Z is a constant that depends on the level of confidence desired. The error estimated from equation 2 gets smaller for larger n and depends on the actual probabilities. Values of Z are predetermined depending on the desired level of confidence. For instance, for a level of confidence of 90%, $Z = 1.64$. The main appeal of formula 2 is that it is easy to understand and use. For instance, if the probability of brittle facies in a cell of the crossplot is 40% and the number of samples is 300, we can say with 90% confidence that the probability is 40% plus or minus 4.6%. This formula, however, is known to fail when the sample is small or when p is near zero or one. Although additional drawbacks with this formula have been well-documented (Brown et al., 2001) and better alternatives do exist, we will still use it to introduce the concept of a margin of error that can be subsequently improved. Other ways to estimate the error can also be used, for instance, analyzing the variance of the results after resampling the input log facies or after repeated blind tests with different horizontal wells.

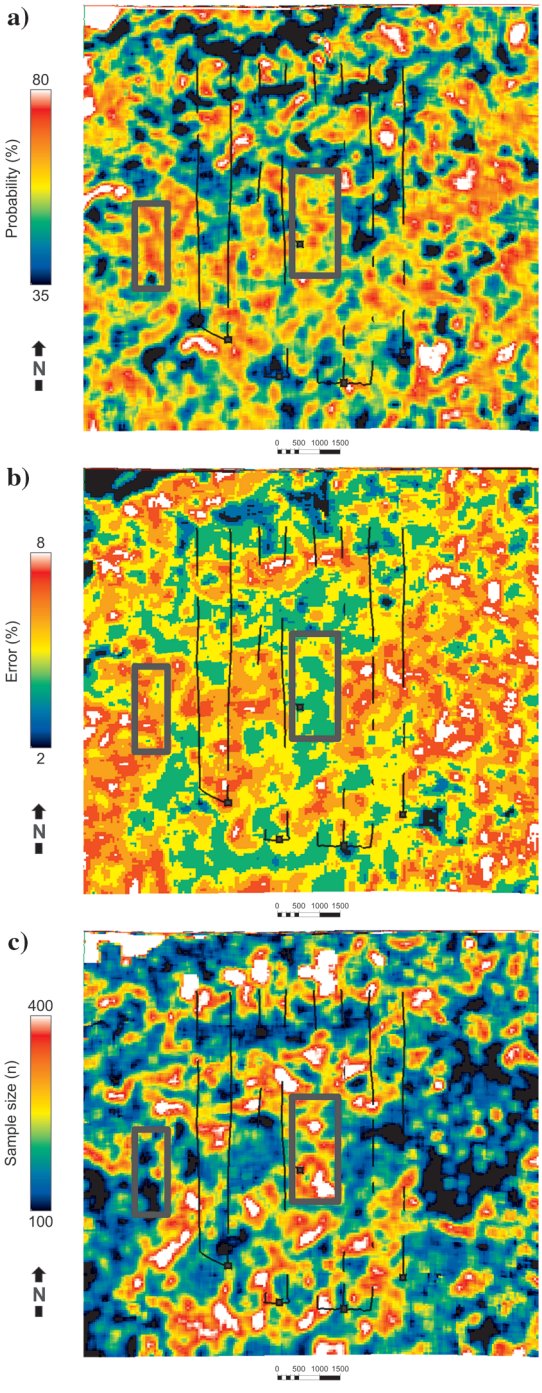

Figure 10. (a) Facies probabilities for a layer close to horizontal well trajectories (map view). (b) Percentage margin of error from equation 2. (c) Sample size. The scales are in feet.

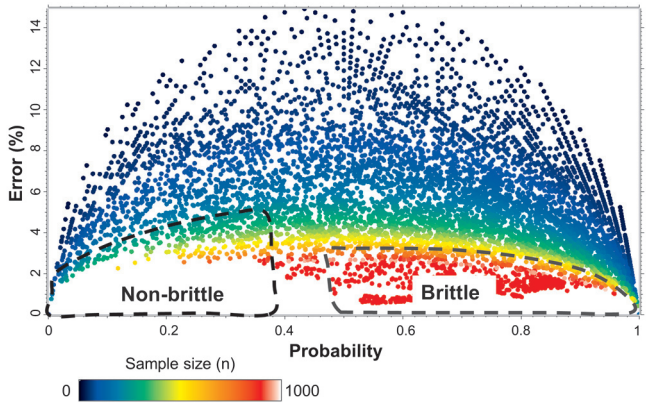

Figure 11. Probability of brittle facies versus margin of error colored by sample size.

The outputs of the facies probability analysis are volumes of probability of brittle/nonbrittle facies, sample size, and margin of error estimated from equation 2. Figure 10 shows an example of the output for a layer near the horizontal well paths. Two areas (gray rectangles) have been highlighted in each map. Although both areas have similar probabilities, the margins of error in each are different.

INTEGRATED STOCHASTIC FACIES MODELING

As mentioned in the previous section, the outputs of the facies probability analysis are volumes of probability of brittle/nonbrittle rock, sample size, and margin of error in each cell of the geologic grid. Although these outputs can be used in different ways to guide the facies modeling, our approach selects only the "best" points from the seismic inversion and uses them as hard constraints. Such points are those with high probability, small margin of error, and large sample size.

We use sequential indicator simulation (SIS) (Journel and Alabert, 1989; Emery, 2004) as the tool for pixel-based, stochastic facies modeling using seismic constraints. The main reason to select SIS over other tools (e.g., object modeling) is that we want to preserve the VPC and do not have enough geologic information to constrain the additional parameters needed to reproduce the expected geomorphology.

The input for SIS consisted of facies flags along the pilot well, facies flags along the horizontal wells, VPC from the pilot well (at grid resolution), and seismic-derived hard constraints from the facies probability analysis. No regional geologic information was used to constrain the results. We used the same variogram parameters for brittle and nonbrittle facies. The variogram was isotopic with a small range (approximately 300 m or 1000 ft) to adequately preserve the seismic imprint in the simulations. The fact that we use more points than the original log facies flags as hard facies constraints makes the simulation results less dependent on the properties of the variograms and the stochastic nature of the modeling. However, the results are strongly dependent on the cutoffs used to select the hard constraints from the facies probabilities. As already pointed out by van Riel et al. (2005), the fewer the number of points we use from the seismic, the easier it is to honor the well data and the VPC. In our approach, only the most likely and most reliable (or best calibrated) facies information from the seismic inversion ends up being used.

Figure 11 shows the relations between the margin of error from equation 2, probability of brittle rock, and sample size. This figure includes all points in the volume of interest. As expected, the margin of error decreases not only with sample size but also as the probability departs from the vicinity of 50%. Because brittle rocks are more abundant than nonbrittle rocks in this area, brittle rocks tend to be better sampled. Therefore, to have an adequate representation of "minority" nonbrittle facies constraints in the model, we will need to allow higher margins of error for nonbrittle rocks as compared with brittle rocks.

Besides probabilities, margins of error, and sample sizes, the selection of the constraints is also weighted by the expected proportion of brittle/nonbrittle facies along the pilot well for each layer of

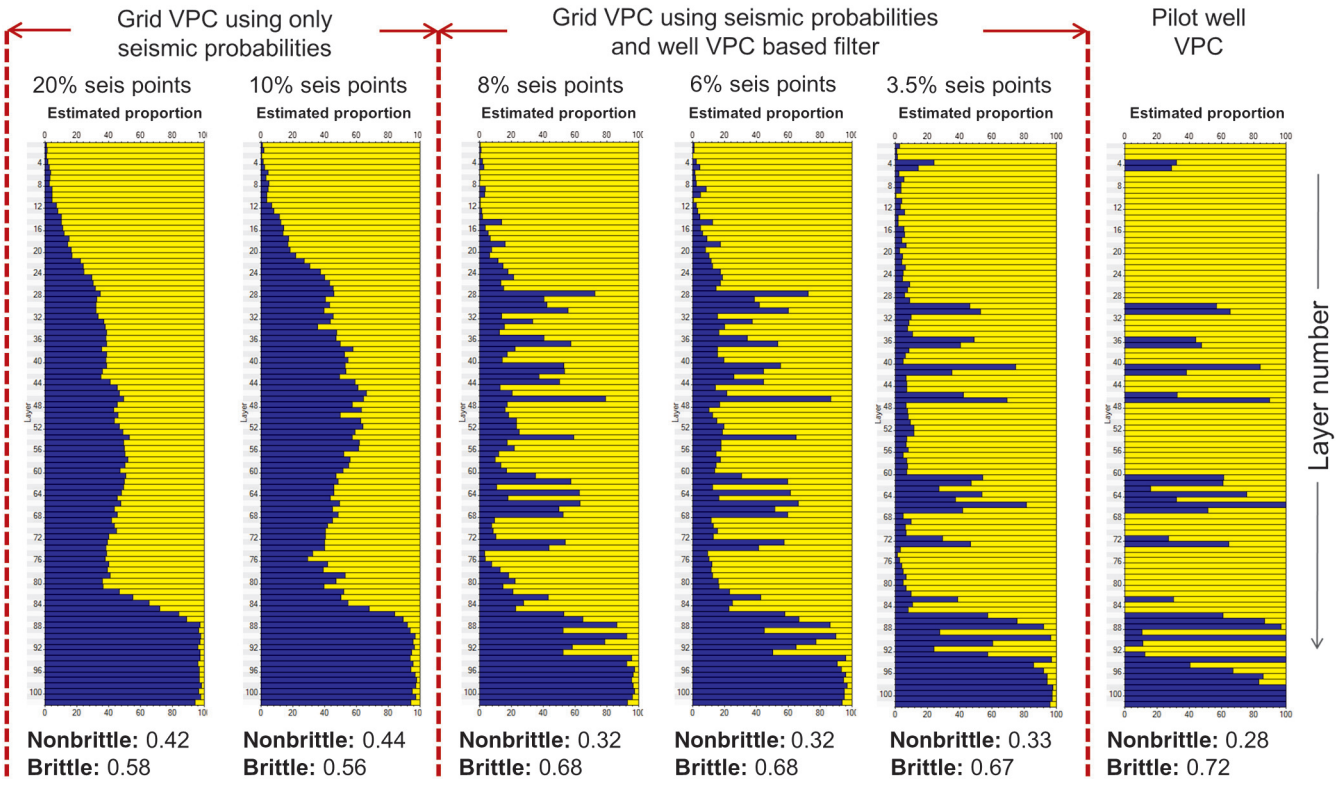

Figure 12. VPC extracted from the grid after stochastic facies simulation using decreasing amounts (from left to right) of seismic-derived hard constraints. The estimated VPC at the pilot well is shown at the right. Brittle/nonbrittle proportions of facies for the whole grid are shown at the bottom of each VPC. The final iteration used only 3.5% of the points in the grid to constrain the facies model. The grid consists of 102 layers of 0.6 m (2 ft) average thickness.

the grid. Figure 12 shows this process in detail. The curve at the right is the VPC at the pilot. The curves at the left of the figure represent the grid VPCs after selecting points with high probability and high reliability from the facies probabilities volume. Notice that the grid VPCs on the left of the figure do not honor the details of the pilot well VPC even if we tighten the error and probability cutoffs and reduce the number of hard data constraints from the seismic. To enhance the match between the grid VPC and pilot well VPC, we weight the selection of the points by the expected proportion observed at the pilot well VPC and further modify the cutoffs related to the brittle/nonbrittle regions in Figure 11. After several iterations of adjusting the selected brittle/nonbrittle regions (which results in further reduction in the number of hard constraints), we are able to generate a model whose VPC is very close to the expected VPC at the pilot well. To have a perfect match of the pilot well VPC in layers that show 100% brittle facies, we would need to eliminate all the lateral variability introduced by the seismic data in those layers. For this reason, we accept a less-than-perfect match. For the final iteration, the selected brittle facies probabilities are higher than 60%, margins of error are less than 3%, and sample sizes are greater than 135 points per cell. For the selected nonbrittle facies, probabilities are less than 30%, margins of error are less than 5%, and sample sizes are greater than 60. Only 3.5% of points in the grid meet either of these requirements.

The VPC assumes stationarity in the area of interest (Yarus et al., 2012). If data from more wells indicate that facies variability that cannot be captured with a single VPC, local proportion curves should be created among groups of wells that are comparable to avoid introducing erroneous trends. In this regard, our method suffers from the same limitations of conventional geostatistical modeling that uses VPCs to constrain facies distribution in areas of strong lateral variability of facies.

Restricting the use of seismic-derived facies only to points with high probability and small margin of error is equivalent to using facies that are well-separated in crossplots of inverted elastic properties. In the context of our methodology, the final cutoffs on probability, margin of error, and sample size give a precise, quantitative meaning to the expression "well-separated." Even if there is total overlap in the elastic properties of facies, we may still be able to pick the most likely facies by estimating a probability and margin

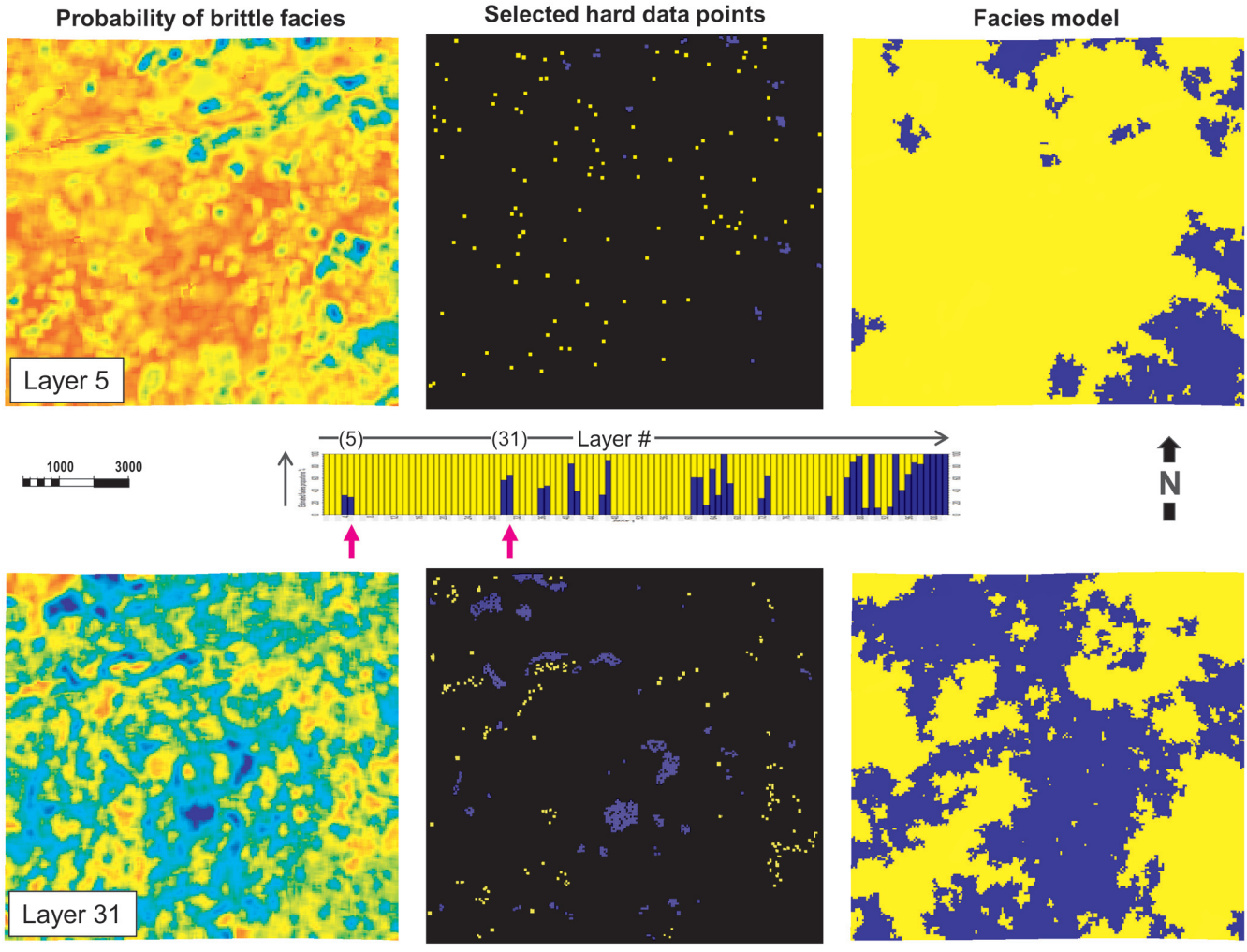

Figure 13. Examples of seismic hard data points extracted from probabilities of britle/nonbrittle facies and used to guide facies modeling in two layers of the geologic model. The pilot well VPC is shown in the middle. Proportions of the modeled facies correspond to proportions in layers indicated by magenta arrows in the pilot well VPC. The scale is in feet.

of error in the same way as opinion polls can indicate who may win a presidential race in states where candidates enjoy comparable support. The tighter the race, the larger the unbiased sample size required to increase the confidence in the prediction.

Figure 13 shows an example of how the seismic constraints guide the facies distribution in two layers of the geologic model. The probability of brittle facies is shown at the left. The selected hard constraints for brittle/nonbrittle facies are shown in the middle. The final facies models after SIS are shown at the right. Notice how the main trends from the seismic data are preserved in the final facies models while still honoring the expected proportion curve at each layer. By selecting only the most likely and reliable points and weighting their selection also by the VPC at the pilot well, we are able to impose seismic trends in the result that honor the facies along horizontals and pilot well data in addition to the VPC.

Figure 14a shows one stochastic realization of the brittle/nonbrittle facies model that results from this workflow. This model is useful in and of itself because brittle facies may be the target for future horizontal drilling. However, if the final goal is to model the original packstone, mudstone, tight carbonate, and clay facies, we can use the brittle/nonbrittle regions in Figure 14a to guide the modeling of the original facies while still honoring their facies flags and VPC along the pilot well. The result is shown in Figure 14b. This transformation from two to four facies is of course nonunique, but it can be useful to test different scenarios of facies-controlled properties such as porosity and permeability.

DISCUSSION

Our workflow to model facies in unconventional reservoirs consists of three integrated steps related to petrophysics, geophysics, and geologic modeling that are summarized in Figure 15. At the heart of our approach are the estimation of facies probabilities from prestack inversion results (red entries in Figure 15) and the iterative selection of seismic-derived hard constraints to guide the facies modeling (the green entries in Figure 15).

Regarding the facies probability estimation, our goal is not to do a detailed comparison of our poll-like approach versus the most commonly used Bayesian approach. Discussions between those who prefer frequencies (or proportions) and those who prefer Bayes have been controversial in other areas of statistical inference, and there is definitely room for discussion about this topic among geophysicists. However, we can mention a fundamental difference between the two approaches that clearly stands out: how prior information is handled. Polls are designed to be a snapshot of the public opinion and they do not know anything about history. They do show how things are with respect to the poll question (within the margin of error), and they do not pretend to speculate about what should be based on our prior knowledge. In this regard, our method for facies probability estimation explores the actual relations between states (ranges of elastic attributes) and responses (facies) regardless of any preconceived notion we may have about what these relations should be. The Bayesian formalism, on the contrary, does allow the integration of prior notions coming from different data types. Having said this, we should emphasize that we do use prior information as a constraint in our workflow but only after facies probabilities have been estimated from seismic data. First, we introduce it in the form of conceptual rock-physics constraints to as-

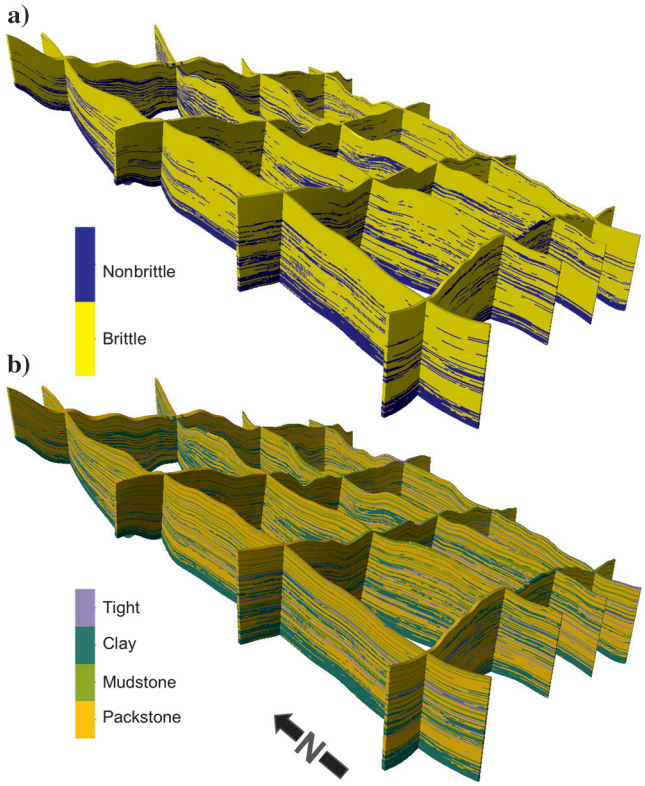

Figure 14. (a) Stochastic realization of brittle/nonbrittle facies using the workflow presented in this paper. (b) Stochastic realization of original facies along brittle (tight, mudstone, and packstone) and nonbrittle (clay) regions of model on (a).

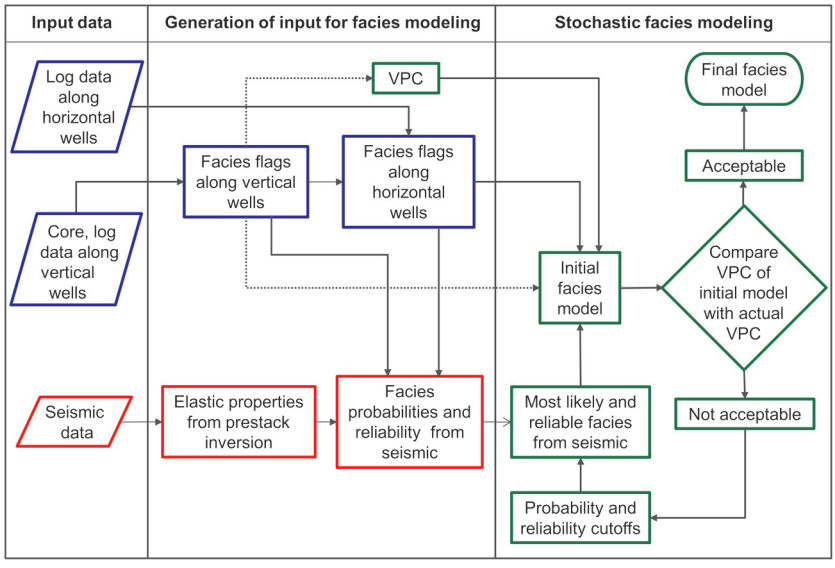

Figure 15. Workflow of the proposed facies modeling in unconventional reservoirs. Different colors around input data or partial results indicate petrophysics (blue), seismic (red), or geomodeling (green) steps.

sign facies to ranges of attributes beyond the ranges of attributes sampled along the well paths. Then, we use it in the stochastic modeling step by attempting to honor the log facies as well as the VPC along the pilot well.

If the data are insufficient or if the sample is biased, polls can be misleading and yield erroneous predictions (as clearly demonstrated, e.g., in the 2015 general election in the United Kingdom or in the 2016 presidential election in the United States). Our method is not exempted from this limitation. In these situations, prior information derived from geologic/geophysical concepts or independent data becomes critical to complement or solve data deficiencies and the Bayesian formalism provides an adequate avenue to address these issues. As pointed out by Bayarri and Berger (2004) among many others, frequentists and Bayesian approaches are not mutually exclusive and should be used in conjunction. A good example of this synergy comes from the area of political sciences. For the problem of forecasting presidential elections, Lizer (2013) proposes to unify historical models based on previous voting patterns with abundant state level opinion polls by using Bayesian forecasting models. The data problems he describes are very similar to what we observe in our crossplots of elastic properties, that is, gaps in the data, polls more abundant in competitive "battleground" states than in less-competitive states, fluctuations in preferences from poll to poll due to sampling differences, among others. Linzer uses polling information to detect trends in the electorate and correct historical forecasts to predict a winner. As we can see, forecasting of presidential elections (or other opinion polls) and facies estimation from seismic data are totally unrelated problems that share analogous goals and methods to achieve them.

Although seismic processing errors may impact the results significantly because they affect the input for the analyses, other errors that have to do with small imprecisions and inaccuracies in seismic well ties may be compensated by using a more robust estimate from hundreds of thousands of points along the horizontals rather than just hundreds of points along the vertical wells.

CONCLUSION

We have presented the application of a new facies modeling workflow in unconventional reservoirs that addresses the petrophysics, rock physics, seismic calibration, and stochastic modeling challenges created by the abundance of long horizontal wells with limited log data. The common practice of discarding the information along horizontals as not usable may result in poorly calibrated facies models. In the example presented in this paper, the number of samples along the eight horizontal wells in the area of interest is more than two orders of magnitude higher than the number samples along the vertical pilot well and yields a more robust calibration when the horizontals are used.

We start by defining facies using LWD GR curves along the horizontals that have been previously calibrated along the pilot well with core data and a full set of logs. The information needed to calibrate the facies along the horizontals to the elastic properties of the reservoir is extracted from the prestack seismic inversion results along the well paths after time-depth conversion constrained by geosteering information. By using crossplots of inverted elastic properties colored by log facies, we estimate facies probabilities and their reliability using a poll-like, frequentist approach instead of the more commonly used Bayesian approach for facies probability estimation. Margins of error in the probabilities are also estimated, and only the most likely and most reliable information from seismic is used to constrain the stochastic facies models. Although no prior facies probabilities are used in the estimation of probabilities from inversion results, we do use and honor prior probabilities in the form of a VPC and log facies in the final facies modeling.

ACKNOWLEDGMENTS

We thank BHP Billiton Petroleum for permission to publish these results and M. Florez for his support during this project. Thanks also to our colleague M. Uland for the petrophysics modeling and log normalization. Detailed comments and numerous suggestions from anonymous reviewers helped to clarify important aspects of the methodology and improved the overall quality of the paper.

REFERENCES

Bayarri, M. J., and J. O. Berger, 2004, The interplay of Bayesian and frequentist analysis: Statistical Science, **19**, 58–80, doi: 10.1214/088342304000000116.

Brown, L. D., T. T. Cai, and A. DasGupta, 2001, Interval estimation for a binomial proportion: Statistical Science, **16**, 101–133, doi: 10.1214/ss/1009213286.

Emery, X., 2004, Properties and limitations of sequential indicator simulation: Stochastic Environmental Research and Risk Assessment, **18**, 414–424, doi: 10.1007/s00477-004-0213-5.

Grana, D., T. Mukerji, J. Dvorkin, and G. Mavko, 2012, Stochastic inversion of facies from seismic data based on sequential simulations and probability perturbation method: Geophysics, **77**, no. 4, M53–M72, doi: 10.1190/geo2011-0417.1.

Jordan, D. L., and D. J. Goggin, 1995, An application of categorical indicator geostatistics for facies modeling in sand-rich turbidite systems: Annual Technical Conference and Exhibition, SPE, doi: 10.2118/30603-MS.

Journel, A. G., and F. Alabert, 1989, Non-Gaussian data expansion in the earth sciences: Terra Nova, **1**, 123–134, doi: 10.1111/j.1365-3121.1989.tb00344.

Lizer, D. A., 2013, Dynamic Bayesian forecasting of presidential elections in the states: Journal of the American Statistical Association, **108**, 124–134, doi: 10.1080/01621459.2012.737735.

Michelena, R. J., K. S. Godbey, and P. E. Rodrigues, 2011, Facies probabilities from multidimensional crossplots of seismic attributes: Application to tight gas Mamm Creek Field, Piceance Basin, Colorado: The Leading Edge, **30**, 62–69, doi: 10.1190/1.3535434.

Mukerji, T., P. Avseth, G. Mavko, I. Takahashi, and E. Gonzalez, 2001, Statistical rock physics: Combining rock physics, information theory, and geostatistics to reduce uncertainty in seismic reservoir characterization: The Leading Edge, **20**, 313–319, doi: 10.1190/1.1438938.

Ravenne, C., A. Galli, B. Doligez, H. Beucher, and R. Eschard, 2002, Quantification of facies relationships via proportion curves, *in* M. Armstrong, C. Bettini, N. Champigny, A. Galli, and A. Remacre, eds., Geostatistics Rio 2000: Kluwer Academic, 19–40.

Sams, M., I. Millar, W. Satriawan, D. Saussus, and S. Bhattacharyya, 2011, Integration of geology and geophysics through geostatistical inversion: A case study: First Break, **29**, 47–56, doi: 10.3997/1365-2397.2011023.

Saussus, D., and M. Sams, 2012, Facies as the key to using seismic inversion for modeling reservoir properties: First Break, **30**, 45–52, doi: 10.3997/1365-2397.2012009.

van Riel, P., P. Mesgad, H. Debeye, and M. Sams, 2005, Full integration of seismic data into geostatistical reservoir modeling, *in* T. C. Coburn, J. M. Yarus, and R. L. Chambers, eds., Stochastic modeling and geostatistics: Principles, methods, and case studies: AAPG Computer Applications in Geology, 207–218.

Yarus, J. M., R. L. Chambers, M. Maucec, and G. Shi, 2012, Facies simulation in practice: Lithotype proportion mapping and Plurigaussian simulation, a powerful combination: Ninth International Geostatistics Congress, P-014.